Journal of Sound and Vibration (2001) **242**(3), 397–409
doi:10.1006/jsvi.2000.3378, available online at http://www.idealibrary.com on IDEAL®

PARAMETRIC INSTABILITY OF POLYGONAL MINDLIN–REISSNER-PLATES SUBJECTED TO HARMONIC IN-PLANE FORCES

M. Baldinger, H. Irschik and A. K. Belyaev

Division of Technical Mechanics, Department of Mechanics and Mechanical Engineering, Altenbergerstr. 69, *Johannes Kepler University of Linz, Linz A*-4040, *Austria.*
E-mail: martin.baldinger@mechatronik.uni-linz.ac.at

(*Received* 3 *December* 1999, *and in final form* 15 *August* 2000)

In this paper, the dynamic stability analysis of shear-deformable plates of arbitrary polygonal planform is performed within the framework of the Mindlin–Reissner theory. The plates are considered to be subjected to a parametric excitation by harmonic in-plane forces. The influence of plate shear and rotatory inertia is taken into account, a two-parameter Pasternak foundation is chosen, and the more accurate theory of Brunelle and Robertson is included. Considering harmonic in-plane forces yields partial differential equations with time-dependent parameters. Ordinary differential equations for the generalized co-ordinates are derived by expanding the deflection and the cross-sectional rotations of the plate in series representations in terms of normal modes and using Galerkin's principle. The normal modes are governed by Helmholtz-eigenvalue problems in the case of simply supported boundaries. Parametric instability of flexural- and thickness-shear motions are studied in more detail. The governing equations enable a number of results to be obtained which reveal the influence of the special shape of the plate domain represented by the Helmholtz eigenvalue, parameters of the foundation and a tracer for the Brunelle and Robertson theory. The main merit of the approach is that the particular shape and mechanical properties of the polygonal plate are represented in these equations in terms of Helmholtz eigenvalues which allows a general analysis for plates of arbitrary polygonal planform to be performed. A vast amount of literature exists on Helmholtz eigenvalues in the context of natural vibrations of membranes, which may be utilized. The boundaries of the principal instability region are calculated and the stability charts of these two motions are represented graphically. These results are finally derived in a non-dimensional form and illustrated by means of numerical examples.

1. INTRODUCTION

Dynamic stability of continuous structures subjected to time-dependent in-plane loads is one of the most interesting problems in the field of structural vibrations. When investigating plates, the motion is reduced to the Mathieu equation which yields the stability charts. Instability here is in the sense that the amplitude of the response increases without limit. The problem was extensively investigated by Bolotin [1] and further results can be found, for example, in the book by Evan-Iwanowski [2].

It has been shown by Irschik [3] that a simply supported polygonal Mindlin plate has three types of eigenmotions with corresponding spectra of eigenfrequencies and buckling eigenvalues, which are related to Dirichlet's and Neumann's Helmholtz-type eigenvalue problems. These eigenvalue problems have a mechanical interpretation as natural vibrations of prestressed membranes with fixed or vertically sliding edges respectively. No

0022-460X/01/180397 + 13 $35.00/0

previous attempt has been made to determine the importance of the principal instability regions associated with these modes and the influence of the corresponding Helmholtz eigenvalue.

The present study thus covers an existing gap in the understanding of the parametric instability of continuous systems with respect to the above class of simply supported arbitrary polygonal plates. The analysis is based on Galerkin's principle and the governing equations are obtained by satisfying the orthogonality relations of the natural modes. These equations are used to analyze the stability behaviour of the above plates.

The paper is organized as follows. The governing equations for flexural vibrations of moderately thick plates, considering transverse inertia, rotatory inertia, shear and neglecting in-plane inertia, are derived in section 2 from Mindlin's theory, which is also referred to as the Reissner–Mindlin theory because of Reissner's celebrated preliminary work. These are differential equations of sixth order in terms of the plate deflection and the cross-sectional rotations. The boundary conditions for straight and simply supported Mindlin plates of polygonal shape are obtained. Section 3 deals with the eigenvalue analysis of a simply supported polygonal plate. The plate is shown to have three decoupled types of eigenmotion, each of them being governed by an uncoupled boundary-value problem of the Helmholtz type. These uncoupled eigenmotions govern flexural, thickness-shear and thickness-twist motions of the plate. Dynamic stability of a simply supported polygonal plate subjected to a harmonic in-plane force is analyzed in section 4. Expanding in terms of normal modes and applying the principle of virtual work yields three coupled differential equations of Mathieu type for generalized co-ordinates. The main merit of the approach becomes evident as one observes that the particular shape and mechanical properties of the polygonal plate are represented in these equations in terms of Helmholtz eigenvalues. This allows one to perform a general analysis for polygonal plates of arbitrary shape. The remainder of section 4 is devoted to deriving a closed-form expression for the boundaries of the principal instability region. Some typical instability regions are displayed in section 5.

2. BOUNDARY-VALUE PROBLEM FOR VIBRATION OF MINDLIN'S POLYGONAL PLATES

When describing the dynamic problems of polygonal plates, Mindlin's plate theory [4] is significant. Inserting Mindlin's kinematic assumption and the constitutive equations into the equations of motion for moderately thick plates, considering the effects of transverse inertia, rotatory inertia and shear, and neglecting in-plane inertia, yields a system of three differential equations of sixth order in terms of the plate deflection w and the cross-sectional rotations ψ_x and ψ_y, [4, 5]. The midplane of the plate is assumed to lie in the x–y plane, the z-axis points downwards (Figure 1).

Taking into account a two-parameter Pasternak foundation [6], Mindlin's extended equations read as

$$\frac{K}{2}\left[(1-\nu)\Delta\psi_x + (1+\nu)\frac{\partial\phi}{\partial x}\right] - \kappa^2 Gh\left(\frac{\partial w}{\partial x} + \psi_x\right) = \frac{\rho h^3}{12}\frac{\partial^2\psi_x}{\partial t^2} - \frac{ch^2}{12}\left(n_x\frac{\partial^2\psi_x}{\partial x^2} + 2n_{xy}\frac{\partial^2\psi_x}{\partial x\partial y} + n_y\frac{\partial^2\psi_x}{\partial y^2}\right), \tag{1a}$$

$$\frac{K}{2}\left[(1-\nu)\Delta\psi_y + (1+\nu)\frac{\partial\phi}{\partial y}\right] - \kappa^2 Gh\left(\frac{\partial w}{\partial y} + \psi_y\right) = \frac{\rho h^3}{12}\frac{\partial^2\psi_y}{\partial t^2} - \frac{ch^2}{12}\left(n_x\frac{\partial^2\psi_y}{\partial x^2} + 2n_{xy}\frac{\partial^2\psi_y}{\partial x\partial y} + n_y\frac{\partial^2\psi_y}{\partial y^2}\right), \tag{1b}$$

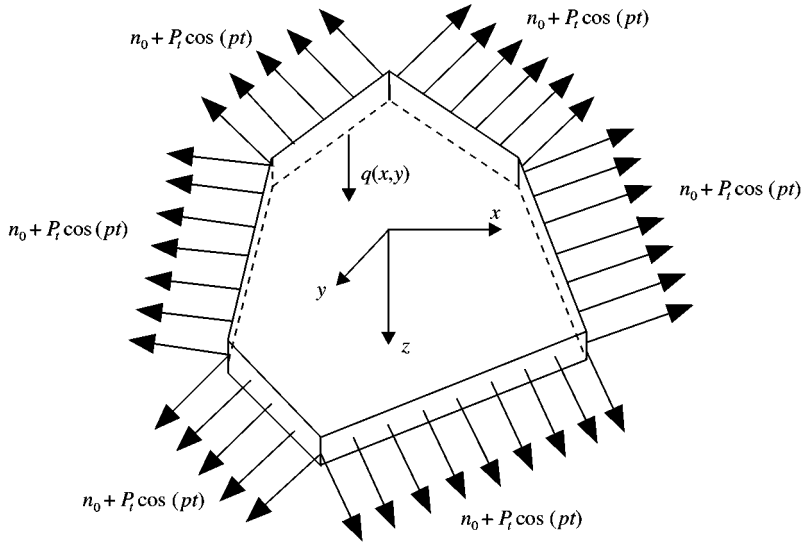

Figure 1. Plate with acting in-plane forces.

$$\kappa^2 Gh(\Delta w + \phi) + q = \rho h \frac{\partial^2 w}{\partial t^2} - \left(n_x \frac{\partial^2 w}{\partial x^2} + 2n_{xy} \frac{\partial^2 w}{\partial x \partial y} + n_y \frac{\partial^2 w}{\partial y^2} \right), \tag{1c}$$

where the two-dimensional Laplace operator Δ and the operator ϕ are defined as follows:

$$\Delta(\ ) := \frac{\partial^2(\ )}{\partial x^2} + \frac{\partial^2(\ )}{\partial y^2}, \quad \phi := \frac{\partial \psi_x}{\partial x} + \frac{\partial \psi_y}{\partial y}. \tag{2}$$

In equation (1), the influence of shear is characterized by $s = 1/\kappa^2 Gh$ with the shear factor κ^2. The coefficient of rotatory inertia is denoted by $r = \rho h^3/12$ and $K = Eh^3/12(1 - \nu^2)$ is the bending stiffness. A possible lateral loading q is considered in addition, which in the present case is attributed to the reaction forces of the Pasternak foundation, $q = -\mathrm{d}w + e\Delta w$. Here d and e are Pasternak's foundation parameters [6]. The terms with the tracer c in equations (1(a) and (b)), known as the "curvature terms", are due to Brunelle and Robertson [7]. These terms reflect the influence of the in-plane forces according to the Trefftz theory of elastic bodies under initial stress. With $c = 1$ the Brunelle–Robertson theory is a generalization of the Herrmann–Armenakas theory [8], in with $c = 0$. In the following, in-plane forces of the hydrostatic type, $n_x = n_y = n = n_0 + P_t \cos(pt)$, $n_{xy} = 0$, are considered (see Figure 1).

The boundary conditions for straight and simply supported shear-deformable plates of polygonal shape are cast in the form

$$\Gamma: w = 0$$
$$m_n + \frac{ch^2}{12}(n_0 + P_t \cos(pt)) \frac{\partial \psi_n}{\partial n} = K\left(\frac{\partial \psi_n}{\partial n} + \nu \frac{\partial \psi_s}{\partial s} \right) + \frac{ch^2}{12}(n_0 + P_t \cos(pt)) \frac{\partial \psi_n}{\partial n} = 0,$$

$$\psi_s = 0. \tag{3}$$

Here n and s denote, respectively, the normal and tangential unit vectors of the local co-ordinate system on the border Γ, and m_n is the bending moment.

3. EIGENVALUE ANALYSIS

The above problem for simply supported polygonal plates has three decoupled types of eigenmotion, all of them are governed by uncoupled boundary value problems of the Helmholtz type. In the following, the mean in-plane force n_0 in the eigenvalue analysis, for details of the derivation are included (see Irschik [3]).

3.1. FLEXURAL MOTION

The flexural eigenfunctions $w_{\nu 1}$ with the corresponding eigenfrequencies $\omega_{\nu 1}$ are governed by the following Helmholtz-eigenvalue problem with Dirichlet's boundary conditions:

$$\Delta w_{\nu 1} + \alpha_{\nu 1} w_{\nu 1} = 0, \quad \Gamma : w_{\nu 1} = 0, \tag{4}$$

where $\alpha_{\nu 1}$ are the Helmholtz eigenvalues ($\nu = 1, 2, 3, \ldots, \infty$). The cross-sectional rotations of the flexural mode are related to $\omega_{\nu 1}$ and $\alpha_{\nu 1}$ by

$$\psi_{x\nu 1} = \varepsilon_{\nu 1} \frac{\partial w_{\nu 1}}{\partial x}, \quad \psi_{y\nu 1} = \varepsilon_{\nu 1} \frac{\partial w_{\nu 1}}{\partial x},$$

where

$$\varepsilon_{\nu 1} = -\left[\left(1 + \frac{n_0 + e}{\kappa^2 \mathrm{Gh}}\right) - \frac{(\rho h \omega_{\nu 1}^2 - d)}{\kappa^2 \mathrm{Gh}} \frac{1}{\alpha_{\nu 1}}\right]. \tag{5}$$

The natural frequencies of the flexural motion of Mindlin–Reissner plates in terms of $\alpha_{\nu 1}$ are

$$\omega_{\nu 1}^2 = \Omega^2 \frac{\bar{\beta}_\nu}{2}\left(1 - \left[1 - \frac{4\bar{\gamma}_\nu}{\bar{\beta}_\nu^2}\right]^{1/2}\right), \tag{6}$$

where $\bar{\beta}_\nu$ and $\bar{\gamma}_\nu$ are given by

$$\bar{\beta}_\nu = \beta_\nu + \xi_\nu n_0, \quad \bar{\gamma}_\nu = \gamma_\nu + \xi_\nu n_0 + \eta_\nu n_0^2, \quad \nu = 1, 2, 3, 4, \ldots,$$

$$\beta_\nu = 1 + \alpha_\nu \frac{(e + \mathrm{d}/\alpha_\nu) 1/\Omega^2 + K\rho h s + r}{\rho h}, \quad \gamma_\nu = \alpha_\nu \frac{[(e + \mathrm{d}/\alpha_\nu)(1 + Ks\alpha_\nu) + K\alpha_\nu]}{\rho h \Omega^2},$$

$$\zeta_\nu = \alpha_\nu \left(\frac{1}{\rho h \Omega^2} + \frac{ch^2}{12} s\right), \quad \xi_\nu = \frac{\alpha_\nu [1 + (Ks + ch^2/12)\alpha_\nu]}{\rho h \Omega^2}, \quad \eta_\nu = \frac{(ch^2/12) s \alpha_\nu^2}{\rho h \Omega^{12}}, \tag{7}$$

with the characteristic frequency $\Omega = \sqrt{1/sr}$. The following three kinematic components determine the natural frequencies $\omega_{\nu 1}$ of the flexural motion:

$$\omega_{\nu 1} : w_{\nu 1}, \quad \psi_{x\nu 1} = \varepsilon_{\nu 1} \frac{\partial w_{\nu 1}}{\partial x}, \quad \psi_{y\nu 1} = \varepsilon_{\nu 1} \frac{\partial w_{\nu 1}}{\partial y}. \tag{8}$$

3.2. THICKNESS-SHEAR MOTION

The eigenfunctions w_{v2} of the thickness-shear mode with the corresponding frequencies ω_{v2} are also governed by a Helmholtz-eigenvalue problem with Dirichlet's boundary conditions:

$$\Delta w_{v2} + \alpha_{v2} w_{v2} = 0, \quad \Gamma : w_{v2} = 0, \tag{9}$$

where α_{v2} are the Helmholtz eigenvalues ($v = 1, 2, 3, \ldots, \infty$). The cross-sectional rotations of the thickness-shear mode are related to ω_{v2} and α_{v2} by

$$\psi_{xv2} = \varepsilon_{v2} \frac{\partial w_{v2}}{\partial x}, \quad \psi_{yv2} = \varepsilon_{v2} \frac{\partial w_{v2}}{\partial y},$$

where

$$\varepsilon_{v2} = -\left[\left(1 + \frac{n_0 + e}{\kappa^2 \mathrm{Gh}}\right) - \frac{(\rho h \omega_{v2}^2 - d)}{\kappa^2 \mathrm{Gh}} \frac{1}{\alpha_{v2}}\right]. \tag{10}$$

The natural frequencies of the thickness-shear motion of Mindlin–Reissner plates in terms of α_{v2} are

$$\omega_{v2}^2 = \Omega^2 \frac{\bar{\beta}_v}{2}\left(1 + \left[1 - \frac{4\bar{\gamma}_v}{\bar{\beta}_v^2}\right]^{1/2}\right), \tag{11}$$

where $\bar{\beta}_v$ and $\bar{\gamma}_v$ are given by equations (7). The natural frequencies ω_{v2} of the thickness-shear motion are associated with the following components

$$\omega_{v2} : w_{v2}, \quad \psi_{xv2} = \varepsilon_{v2} \frac{\partial w_{v2}}{\partial x}, \quad \psi_{yv2} = \varepsilon_{v2} \frac{\partial w_{v2}}{\partial y}. \tag{12}$$

The eigenvalue problems, equations (4) and (9) are identical. So the Helmholtz eigenvalues and the eigenfunctions of these two modes are equal. These two modes differ only in the natural frequencies and the factors of the cross-sectional rotations (cf. equations (6) and (11)),

$$\alpha_{v1} = \alpha_{v2}, \quad w_{v1} = w_{v2}, \quad \omega_{v1} \neq \omega_{v2}, \quad \varepsilon_{v1} \neq \varepsilon_{v2}. \tag{13}$$

Note that, due to their importance with respect to membrane vibrations, a vast amount of literature exists on Helmholtz eigenvalues in polygonal domains (e.g., Leissa [9]).

3.3. THICKNESS-TWIST MOTION

The transverse displacement of the thickness-twist mode vanishes, $w_{v3} = 0$, $v = 1, 2, 3, \ldots, \infty$. The cross-sectional rotations of this mode are given by the following expressions:

$$\psi_{xv3} = -\frac{1}{\alpha_{v3}} \frac{\partial H_v}{\partial y}, \quad \psi_{yv3} = \frac{1}{\alpha_{v3}} \frac{\partial H_v}{\partial x}. \tag{14}$$

Now there is an eigenvalue problem with Neumann's boundary conditions for H_v, which can be treated separately from w_{vi},

$$\Delta H_v + \alpha_{v3} H_v = 0, \quad \Gamma : \frac{\partial H_v}{\partial n} = 0. \tag{15}$$

The corresponding eigenvalues are α_{v3} ($v = 1, 2, 3, \ldots, \infty$). The natural frequencies of the thickness-twist mode follow from

$$\omega_{v3}^2 = \frac{\alpha_{v3}[K(1-v)/2 + (ch^2/12)n_0] + \kappa^2 \mathrm{Gh}}{\rho h^3/12}. \tag{16}$$

Thus, the eigenfrequencies of the thickness-twist motion are determined by the following three kinematic components:

$$\omega_{v3} : w_{v3} = 0, \quad \psi_{xv3} = -\frac{1}{\alpha_{v3}}\frac{\partial H_v}{\partial y}, \quad \psi_{yv3} = \frac{1}{\alpha_{v3}}\frac{\partial H_v}{\partial x}. \tag{17}$$

4. SOLUTION CONCEPT FOR DYNAMIC STABILITY ANALYSIS

When investigating the dynamic stability of a polygonal plate with simply supported boundary conditions and neglecting the effect of in-plane inertia, the parametric excitation is modelled by time-harmonic in-plane forces of the form $n(x, y, t) = n_0 + P_t \cos(pt)$ (see reference [1] for principles of the dynamic stability analysis). The following application to Mindlin plates has been the content of the doctoral thesis of the first author [10]. Here n_0 is the mean normal force and spacewise constant, P_t is the amplitude of the parametric excitation and also space-wise constant, and p is the excitation frequency.

4.1. EXPANSION INTO NORMAL MODES

As the problem is linear, the cross-sectional rotations $\psi_x^*(x, y, t)$ and $\psi_y^*(x, y, t)$ and the deflection $w^*(x, y, t)$ can be put in the form

$$\psi_x^*(x, y, t) = \sum_{v=1}^{\infty} \varepsilon_{v1} Q_{v1}(t) \frac{\partial w_{v1}(x, y)}{\partial x} + \sum_{v=1}^{\infty} \varepsilon_{v2} Q_{v2}(t) \frac{\partial w_{v2}(x, y)}{\partial x} - \sum_{v=1}^{\infty} \frac{1}{\alpha_{v3}} Q_{v3}(t) \frac{\partial H_v(x, y)}{\partial y},$$

$$\psi_y^*(x, y, t) = \sum_{v=1}^{\infty} \varepsilon_{v1} Q_{v1}(t) \frac{\partial w_{v1}(x, y)}{\partial y} + \sum_{v=1}^{\infty} \varepsilon_{v2} Q_{v2}(t) \frac{\partial w_{v2}(x, y)}{\partial y} + \sum_{v=1}^{\infty} \frac{1}{\alpha_{v3}} Q_{v3}(t) \frac{\partial H_v(x, y)}{\partial x},$$

$$w^*(x, y, t) = \sum_{v=1}^{\infty} (Q_{v1}(t) w_{v1}(x, y) + Q_{v2}(t) w_{v2}(x, y)), \tag{18}$$

where ε_{v1}, ε_{v2} and α_{v3} are given by equations (5), (10) and (16). The Q_{vi}'s are the generalized co-ordinates of the first, second and third eigenfunctions respectively, and $w_{v1}(x, y)$, $w_{v2}(x, y)$ and $H_v(x, y)$ are the normalized eigenmode functions of a polygonal plate.

Inserting expressions (18) into the equations of motion (1) gives residual external moments and forces, which are marked by a superscript $*$:

$$\sum_{v=1}^{\infty} \left[M_{v1} \frac{\partial w_{v1}}{\partial x} + M_{v2} \frac{\partial w_{v2}}{\partial x} - M_{v3} \frac{\partial H_v}{\partial y} \right] = m_y^*,$$

$$\sum_{v=1}^{\infty} \left[M_{v1} \frac{\partial w_{v1}}{\partial y} + M_{v2} \frac{\partial w_{v2}}{\partial y} + M_{v3} \frac{\partial H_v}{\partial x} \right] = m_x^*, \quad \sum_{v=1}^{\infty} [F_{v1} w_{v1} + F_{v2} w_{v2}] = q^*. \tag{19}$$

The notation in equation (19) is as follows:

$$M_{vi} = (\ddot{Q}_{vi} + \omega_{vi}^2 Q_{vi}) \frac{\rho h^3}{12} \varepsilon_{vi} + \frac{ch^2}{12} \varepsilon_{vi} \alpha_{vi} P_t \cos(pt) Q_{vi}, \quad i = 1, 2,$$

$$M_{v3} = (\ddot{Q}_{v3} + \omega_{v3}^2 Q_{v3}) \frac{\rho h^3}{12} \frac{1}{\alpha_{v3}} + \frac{ch^2}{12} P_t \cos(pt) Q_{v3},$$

$$F_{vi} = (\ddot{Q}_{vi} + \omega_{vi}^2 Q_{vi}) \rho h + \alpha_{vi} P_t \cos(pt) Q_{vi}, \quad i = 1, 2. \tag{20}$$

4.2. APPLICATION TO THE PRINCIPLE OF VIRTUAL WORK

Galerkin's principle applied to equations (19) requires that these residual external forces and moments form a self-equilibrating set. The application of the principle of virtual work yields

$$\int_\Omega (q^* \delta w^* + m_x^* \delta \psi_x^* + m_y^* \delta \psi_y^*) \, \mathrm{d}\Omega = 0. \tag{21}$$

The expressions (18), being a linear combination of the eigenfunctions, satisfy all the boundary conditions (3). For this reason, no residual forces and moments at the boundary need to be considered. Inserting the virual displacements and rotations

$$\delta w^* = \sum_{k=1}^{\infty} (w_{k1} \delta Q_{k1} + w_{k2} \delta Q_{k2}),$$

$$\delta \psi_x^* = \sum_{k=1}^{\infty} \left(\varepsilon_{k1} \frac{\partial w_{k1}}{\partial x} \delta Q_{k1} + \varepsilon_{k2} \frac{\partial w_{k2}}{\partial x} \delta Q_{k2} - \frac{1}{\alpha_{k3}} \frac{\partial H_k}{\partial y} \delta Q_{k3} \right),$$

$$\delta \psi_y^* = \sum_{k=1}^{\infty} \left(\varepsilon_{k1} \frac{\partial w_{k1}}{\partial y} \delta Q_{k1} + \varepsilon_{k2} \frac{\partial w_{k2}}{\partial y} \delta Q_{k2} + \frac{1}{\alpha_{k3}} \frac{\partial H_k}{\partial x} \delta Q_{k3} \right), \tag{22}$$

into Galerkin's principle, integrating by part, using the Green and the Gauss formulae, together with the orthogonal relations of the natural modes leads to the following equations (see Baldinger [10] for details):

$$F_{k1} + F_{k2} + M_{k1} \varepsilon_{k1} \alpha_{k1} + M_{k2} \varepsilon_{k1} \alpha_{k1} = 0,$$

$$F_{k1} + F_{k2} + M_{k1} \varepsilon_{k2} \alpha_{k2} + M_{k2} \varepsilon_{k2} \alpha_{k2} = 0, \quad M_{k3} = 0. \tag{23}$$

Inserting notation (20) and taking into account that $\alpha_{k1} = \alpha_{k2}$, the following three equations for the generalized co-ordinates are reached:

$$(\ddot{Q}_{k1} + \omega_{k1}^2 Q_{k1}) \left[\rho h + \frac{\rho h^3}{12} \varepsilon_{k1}^2 \alpha_{k1} \right]$$

$$+ P_t \cos(pt) \left[\alpha_{k1} \left(\frac{ch^2}{12} \varepsilon_{k1}^2 \alpha_{k1} + 1 \right) Q_{k1} + \alpha_{k2} \left(\frac{ch^2}{12} \varepsilon_{k1} \varepsilon_{k2} \alpha_{k1} + 1 \right) Q_{k2} \right] = 0,$$

$$(\ddot{Q}_{k2} + \omega_{k2}^2 Q_{k2}) \left[\rho h + \frac{\rho h^3}{12} \varepsilon_{k2}^2 \alpha_{k2} \right]$$

$$+ P_t \cos(pt)\left[\alpha_{k1}\left(\frac{ch^2}{12}\,\varepsilon_{k1}\varepsilon_{k2}\alpha_{k2}+1\right)Q_{k1} + \alpha_{k2}\left(\frac{ch^2}{12}\,\varepsilon_{k2}^2\alpha_{k2}+1\right)Q_{k2}\right] = 0,$$

$$(\ddot{Q}_{k3} + \omega_{k3}^2 Q_{k3}) + \frac{c\alpha_{k3}}{\rho h} P_t \cos(pt) Q_{k3} = 0, \tag{24}$$

(see Baldinger and Irschik [11] for the initial description).

Equations (24) indicate that the particular shape and mechanical properties of the plate are reflected in the Helmholtz-eigenvalues α_{ki} and the eigenfrequencies ω_{ki} of the plate. The latter, however, follow from α_{ki} via equations (6) and (11). Note also that the generalized co-ordinate Q_{k3} becomes independent of the parametric excitation in the case of missing curvature terms ($c = 0$).

As shown in Section 3, the potential H represents the thickness-twist motion of the plate. In the present case, this eigenmotion is characterized by the cross-sectional rotations, but there is no deflection of the plate. Therefore, the thickness-twist mode is not studied in the following derivation.

4.3. EQUATIONS GOVERNING THE PARAMETRIC INSTABILITY

Rewriting the first two equations (24) results in the following set of ordinary second order linear differential equations:

$$\ddot{Q}_{k1} + \omega_{k1}^2\left(1 + \frac{A_{k1}}{\omega_{k1}^2} P_t \cos(pt)\right) Q_{k1} + A_{k12} P_t \cos(pt) Q_{k2} = 0,$$

$$\ddot{Q}_{k2} + \omega_{k2}^2\left(1 + \frac{A_{k2}}{\omega_{k2}^2} P_t \cos(pt)\right) Q_{k2} + A_{k21} P_t \cos(pt) Q_{k1} = 0. \tag{25}$$

Equations (25) represent a set of second order linear homogeneous equations with periodic coefficients, referred to as Mathieu differential equations and describe the general case as they contain the tracer c (see equations (26)).

The notation of equation (25) is as follows:

$$A_{k1} = \frac{((ch^2/12)\varepsilon_{k1}^2\alpha_{k1}+1)}{((\rho h^3/12)\varepsilon_{k1}^2\alpha_{k1}+\rho h)}\,\alpha_{k1}, \quad A_{k2} = \frac{((ch^2/12)\varepsilon_{k2}^2\alpha_{k2}+1)}{((\rho h^3/12)\varepsilon_{k2}^2\alpha_{k2}+\rho h)}\,\alpha_{k2},$$

$$A_{k12} = \frac{((ch^2/12)\varepsilon_{k1}\varepsilon_{k2}\alpha_{k1}+1)}{((ph^3/12)\varepsilon_{k1}^2\alpha_{k1}+\rho h)}\,\alpha_{k2}, \quad A_{k21} = \frac{((ch^2/12)\varepsilon_{k1}\varepsilon_{k2}\alpha_{k2}+1)}{((ph^3/12)\varepsilon_{k2}^2\alpha_{k2}+\rho h)}\,\alpha_{k1}. \tag{26}$$

The traces ε_{ki} are given by equations (5) and (10).

4.4. PRINCIPLE PARAMETRIC RESONANCE

Confining attention to the investigation of the principle parametric resonance, the boundaries of the principal instability region are obtained by means of the following substitution (see reference [1]):

$$\mathbf{Q} = \begin{bmatrix} Q_{k1} \\ Q_{k2} \end{bmatrix} = \begin{bmatrix} a_1 \\ a_2 \end{bmatrix} \sin\left(\frac{pt}{2}\right) + \begin{bmatrix} b_1 \\ b_2 \end{bmatrix} \cos\left(\frac{pt}{2}\right), \tag{27}$$

where a_1, a_2, b_1 and b_2 are unknown constants. Substituting equation (27) into equation (25), carrying out the trigonometric transformations and neglecting terms containing higher harmonics, gives the following set of equations for the unknown coefficients a_1, a_2, b_1 and b_2:

$$\left(\left[-\left(\frac{p}{2}\right)^2+\omega_{k1}^2-\frac{A_{k1}P_t}{2}\right]a_1-\frac{A_{k12}P_t}{2}a_2\right)\sin\left(\frac{pt}{2}\right)$$
$$+\left(\left[-\left(\frac{p}{2}\right)^2+\omega_{k1}^2+\frac{A_{k1}P_t}{2}\right]b_1+\frac{A_{k12}P_t}{2}b_2\right)\cos\left(\frac{pt}{2}\right)=0,$$
$$\left(\left[-\left(\frac{p}{2}\right)^2+\omega_{k2}^2-\frac{A_{k2}P_t}{2}\right]a_2-\frac{A_{k21}P_t}{2}a_1\right)\sin\left(\frac{pt}{2}\right)$$
$$+\left(\left[-\left(\frac{p}{2}\right)^2+\omega_{k2}^2+\frac{A_{k2}P_t}{2}\right]b_2+\frac{A_{k21}P_t}{2}b_1\right)\cos\left(\frac{pt}{2}\right)=0. \tag{28}$$

It is obvious that equation (28) will be identically satisfied for a_1, a_2, b_1 and $b_2=0$. This solution corresponds to the case in which traverse vibrations of the plate are absent. Non-zero solutions can be found if equation (28) is considered as a system of homogeneous linear equations with respect to a_1, a_2, b_1 and b_2. This system has a non-trivial solution only if the two determinants composed of the coefficients disappear:

$$\begin{bmatrix}\left[-\left(\frac{p}{2}\right)^2+\omega_{k1}^2-\frac{A_{k1}P_t}{2}\right] & -\frac{A_{k12}P_t}{2}\\ -\frac{A_{k21}P_t}{2} & \left[-\left(\frac{p}{2}\right)^2+\omega_{k2}^2-\frac{A_{k2}P_t}{2}\right]\end{bmatrix}\begin{bmatrix}a_1\\a_2\end{bmatrix}=0,$$

$$\begin{bmatrix}\left[-\left(\frac{p}{2}\right)^2+\omega_{k1}^2+\frac{A_{k1}P_t}{2}\right] & \frac{A_{k12}P_t}{2}\\ \frac{A_{k21}P_t}{2} & \left[-\left(\frac{p}{2}\right)^2+\omega_{k2}^2+\frac{A_{k2}P_t}{2}\right]\end{bmatrix}\begin{bmatrix}b_1\\b_2\end{bmatrix}=0. \tag{29}$$

Expanding the determinants and solving the resulting equations for excitation frequency p two quadratic equations are found:

$$\tfrac{1}{16}p^4+p^2(-\tfrac{1}{4}\omega_{k1}^2-\tfrac{1}{4}\omega_{k2}^2+\tfrac{1}{8}A_{k2}P_t+\tfrac{1}{8}A_{k1}P_t)$$
$$+\omega_{k1}^2\omega_{k2}^2-\tfrac{1}{2}\omega_{k1}^2A_{k2}P_t-\tfrac{1}{2}\omega_{k2}^2A_{k1}P_t+\tfrac{1}{4}A_{k1}A_{k2}P_t^2-\tfrac{1}{4}A_{k12}A_{k21}P_t^2=0,$$
$$\tfrac{1}{16}p^4+p^2(-\tfrac{1}{4}\omega_{k1}^2-\tfrac{1}{4}\omega_{k2}^2-\tfrac{1}{8}A_{k2}P_t-\tfrac{1}{8}A_{k1}P_t)$$
$$+\omega_{k1}^2\omega_{k2}^2+\tfrac{1}{2}\omega_{k1}^2A_{k2}P_t+\tfrac{1}{2}\omega_{k2}^2A_{k1}P_t+\tfrac{1}{4}A_{k1}A_{k2}P_t^2-\tfrac{1}{4}A_{k12}A_{k21}P_t^2=0. \tag{30}$$

Solving these equation for frequency p as a function of the parametric excitation P_t gives the boundaries of the principal instability regions.

4.5. NORMALIZATION OF THE RESULTS OBTAINED

The present analysis has, until now, derived general expressions for the boundaries of the principal instability regions for the flexural and the thickness-shear mode. In order to be able to evaluate the relative importance of the principal instability regions associated with

these two modes, it is necessary to express these regions in terms of some reference parameters coinciding for all modes of vibrations.

Let the following scaling

$$\tilde{\alpha}_{ki} = a^2 \alpha_{ki}, \quad \tilde{h} = \frac{h}{a}, \quad \tilde{d} = \frac{da}{G}, \quad \tilde{e} = \frac{e}{Ga}, \quad \tilde{n}_0 = \frac{n_0}{Ga}, \quad \tilde{P}_t = \frac{P_t}{Ga}, \tag{31}$$

be introduced where a denotes a characteristic length of the considered plate. Now, the boundaries of principal instability regions may be determined and plotted in the parameter space $(\tilde{p}, \tilde{P}_t)$ for various Helmholtz-eigenvalues $\tilde{\alpha}_{ki}$. When considering special polygons, such as rectangular or triangular plates, the Helmholtz-eigenvalues α_{ki} of equation (24) may be obtained by powerful analytical or numerical methods. A vast amount of literature exists on Helmholtz eigenvalues in the context of natural vibrations of membranes, which may be utilized.

5. NUMERICAL ILLUSTRATIONS AND CONCLUSIONS

The numerical results are intended to display the instability regions. Figure 2 depicts the boundaries of the dynamic instability region for various Helmholtz-eigenvalues $\tilde{\alpha}_{ki}$. The inner (left) and the outer (right) domain pertain to stability and instability respectively.

In order to achieve this goal an arbitrary polygonal plate is taken with the thickness ratio $\tilde{h} = 0{\cdot}01$ and the non-dimensional foundation parameters $\tilde{d} = 0{\cdot}2$, $\tilde{e} = 0{\cdot}1$ The Poisson's ratio is chosen to be $\nu = 0{\cdot}312$ and Brunelle and Robertson's curvature term is $c = 1$.

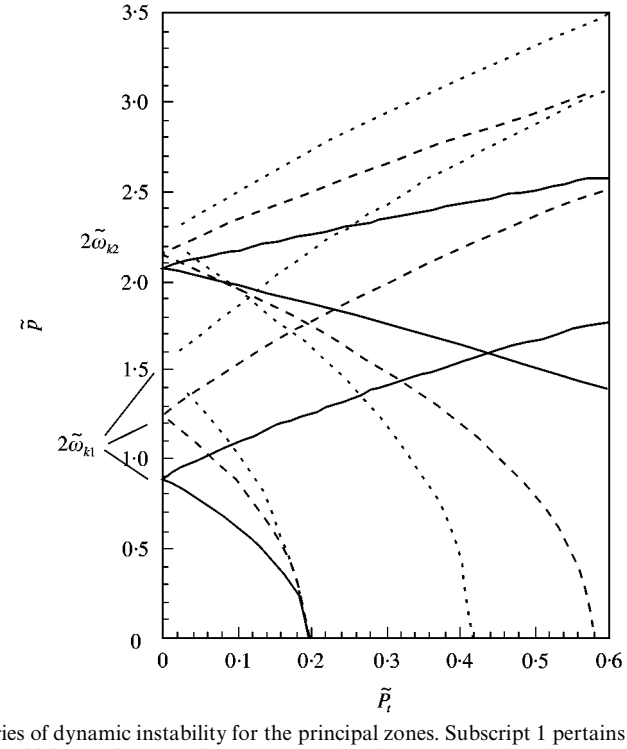

Figure 2. Boundaries of dynamic instability for the principal zones. Subscript 1 pertains to the flexural motion and subscript 2 to the thickness-shear motion: $\tilde{\alpha}_{ki} = 2000$ (——); $\tilde{\alpha}_{ki} = 4000$ (– – –); $\tilde{\alpha}_{ki} = 6000$ (· · · ·).

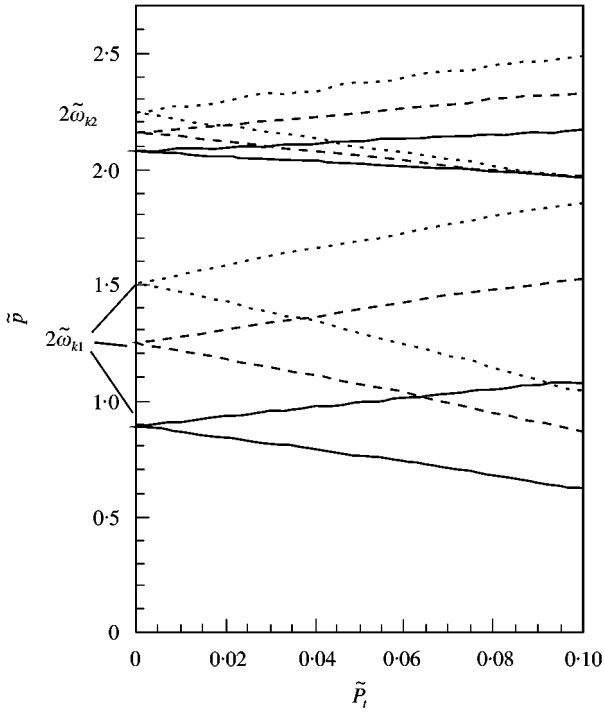

Figure 3. Zoom of the boundaries of dynamic instability for the principle zones. Subscript 1 pertains to the flexural motion and subscript 2 to the thickness-shear motion: $\tilde{\alpha}_{ki} = 2000$ (——); $\tilde{\alpha}_{ki} = 4000$ (– – –); $\tilde{\alpha}_{ki} = 6000$ (· · · ·).

Instability regions for $c = 0$ look quite similar; however, the overlapping of the instability regions occurs at much higher compressive forces, (see Baldinger [10] for details). The shear factor was $\kappa^2 = \frac{5}{6}$ and the non-dimensionalized mean normal force was $\tilde{n}_0 = 0$. High values for $\tilde{\alpha}_{ki}$ were chosen in order to make the effects more apparent.

The instability regions in Figure 2 appear to be shrinking with decreases in parameter $\tilde{\alpha}_{ki}$. These regions are also shifted for lower parameters $\tilde{\alpha}_{ki}$ to the smaller non-dimensional excitation frequency $\tilde{p}$.

The instability regions corresponding to the thickness-shear motion (subscript 2) result in a shift towards higher excitation frequencies. Comparing equations (6) and (11) shows that $\omega_{k2} > \omega_{k1}$.

The range of comparatively low excitation levels is zoomed out in Figure 3. Here the same effects as mentioned above can be seen. The instability regions of these two modes are shown to broaden with the increase in the Helmholtz-eigenvalue $\tilde{\alpha}_{ki}$.

Finally, Figure 4 is a diagram with the non-dimensional ordinate $\tilde{q} = \tilde{p}/2\tilde{\omega}_{k1}$. All boundaries of the flexural motion expand from $\tilde{q} = 1$, whereas the thickness-shear modes expand from $\tilde{q} = \tilde{\omega}_{k2}/\tilde{\omega}_{k1}$.

In considering a plate strip, one arrives at the results for a Timoshenko beam studied by Hagedorn and Koval [12]. For the procedure of this reduction, see Baldinger [10].

Summarizing, the dynamic stability analysis of moderately thick shear-deformable plates of arbitrary polygonal planform within the framework of the concept of Mindlin's theory was proposed. The plates were considered to be subjected to parametric excitation by harmonic in-plane forces. The influence of plate shear and rotatory inertia was taken into account, a two-parameter Pasternak foundation was chosen and the more accurate theory of Brunelle and Robertson was included. Consideration of harmonic in-plane forces lead to

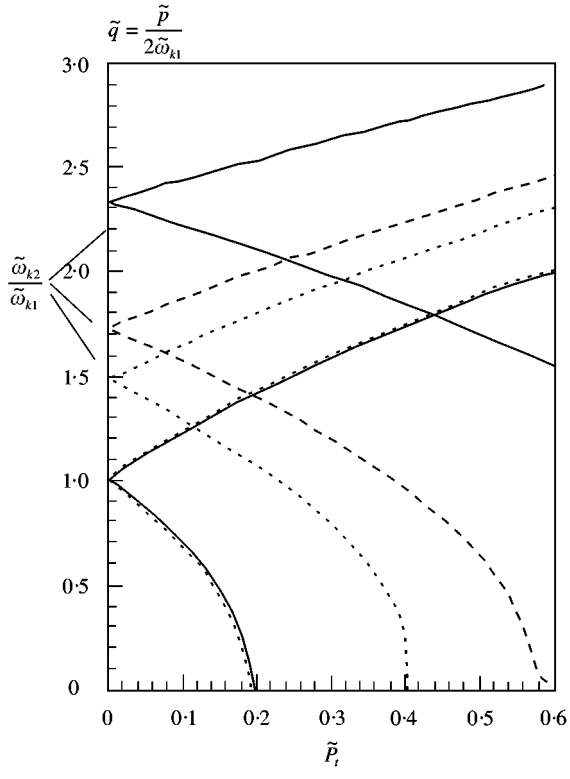

Figure 4. Boundaries of dynamic instability in the plane of non-dimensional parameters $\tilde{q}$ and $\tilde{P}_t$: $\tilde{\alpha}_{ki} = 2000$ (——); $\tilde{\alpha}_{ki} = 4000$ (– – –); $\tilde{\alpha}_{ki} = 6000$ (· · · ·).

partial differential equations with time-dependent parameters which were reduced to ordinary differential equations for the generalized co-ordinates by expanding the deflection and the cross-sectional rotations of the plate in series in terms of normal modes and using Galerkin's principle. Parametric instability of flexural- and thickness-shear motions was studied in more detail. The governing equations allow a number of results to be obtained exposing influence of the special shape of the plate domain represented by the Helmholtz eigenvalue, parameters of the foundation and the tracer for the Brunelle and Robertson theory. The main merit of the approach is that the particular shape and mechanical properties of the polygonal plate are represented in these equations in terms of Helmholtz eigenvalues readily available in the vast literature on membrane vibrations. This enables a general analysis of plates of arbitrary polygonal planform to be performed. The boundaries of the principal instability region were calculated and the stability charts of these two motions were graphically represented. These results are finally derived in a non-dimensional form and illustrated by means of numerical examples. An extension with respect to instability regions of higher order is presently under investigation, and first results have been presented by Baldinger and Irschik [13].

REFERENCES

1. V. V. BOLOTIN 1964 *The Dynamic Stability of Elastic Systems.* New York: Holden-Day.
2. R. M. EVAN-IWANOWSKI 1965 *Applied Mechanical Reviews* **18**, 699–702. On the parametric response of structures.

3. H. IRSCHIK 1985 *Acta Mechanica* **55**, 1–20. Membran-type eigenmotions of Mindlin plates.
4. R. D. MINDLIN 1951 *American Society of Mechanical Engineers Journal of Applied Mechanics* **18**, 31–38. Influence of rotatory inertia and shear on flexural motions of isotropic, elastic plates.
5. E. REISSNER 1985 *American Society of Mechanical Engineers, Applied Mechanics Reviews* **38**, 1435–1464. Reflections on the theory of elastic plates.
6. P. L. PASTERNAK 1954 Fundamentals of a new method of analyzing structures on elastic foundation by means of two foundation moduli. Moskva-Leningrad (in Russian).
7. E. J. BRUNELLE and S. R. ROBERTSON 1974 *American Society of Aeronautics and Astronautics Journal* **12**, 1036–1045. Initially stressed Mindlin plates.
8. G. HERMANN and A. E. ARMENAKAS 1960 *Proceedings American Society of Civil Engineers Journal of the Engineering Mechanics Division* **86**, 65–94. Vibrations and stability of plates under initial stress.
9. A. W. LEISSA 1969 *NASA-SP*-160. Vibrations of Plates.
10. M. BALDINGER 1998 *Ph.D. Thesis Institute of Mechanics and Mechanical Engineering.* Dynamic instability of shearelastic plates (in German).
11. M. BALDINGER and H. IRSCHIK 1998 *ZAMM* **78**, S251–S254. On the parametric stability of Mindlin–Reissner plates subjected to harmonic in-plane forces of the hydrostatic type.
12. P. HAGEDORN and L. R. KOVAL 1971 *Ingenieur-Archiv* **40**, 211–220. On the parametric stability of a Timoshenko beam subjected to a periodic axial load.
13. M. BALDINGER and H. IRSCHIK 1998 In: *Modeling and Simulation Based Engineering*, Vol. **1**, 613–618. Palmdale: Tech Science Press. Regions of dynamic instability of the first and second order for simply supported polygonal Mindlin–Reissner plates.